EPJ Web of Conferences **349**, 01010 (2026) https://doi.org/10.1051/epjconf/202634901010
EMAS 2025

Soft X-ray emission of nickel silicides and nickel aluminides

Xavier Llovet[1*], *Aurélien* Moy[2,3], *Jordi* Ibáñez-Insa[4], and *Philippe* Jonnard[5]

[1]Centres Científics i Tecnològics, Universitat de Barcelona. Lluís Solé i Sabarís, 1-3, 08028 Barcelona, Spain
[2]Gatan, Inc. 5794 W Las Positas Blvd, Pleasanton CA 94588, USA
[3]Dept. of Geoscience, University of Wisconsin-Madison. 1215 West Dayton Street, Madison WI 53706-1692, USA
[4]Geosciences Barcelona (GEO3BCN, CSIC). Lluís Solé i Sabarís, s/n. 08028 Barcelona, Spain
[5]Sorbonne Université, Faculté des Sciences et Ingénierie. UMR CNRS. 4 place Jussieu, 75252 Paris, France

Abstract. Measurements are presented of the Si and Al L X-ray emission bands of Ni silicides ($Ni_{31}Si_{12}$ and Ni_2Si) and Ni aluminides (Ni_2Al_3 and $NiAl_3$). The spectra, obtained with a soft X-ray spectrometer and electron beam excitation, reflect the distribution of Si and Al *s*- and *d*-states in the valence band. The experimental spectra are compared with X-ray emission spectra calculated from the local and partial densities of states obtained with density functional theory.

1 Introduction

Knowledge of the electronic structure of Ni and Al silicides is needed to control their formation and improve their performance. Ni silicides play an important role in semiconductor technology, where they are used as contact materials due to the stability of their properties [1]. Ni aluminides are widely used for high-temperature applications as they have properties that are intermediate between metals and ceramics [2].

Soft X-ray emission spectroscopy (SXES) is known to provide information about the electronic structure of solids [3]. In particular, the measured spectrum is a projection of the density of states of the valence band with respect to atomic site and angular momentum. The application of SXES to the determination of the electronic structure of solids has been a subject of continuing investigations for many years [3]. SXES measurements have generally been carried in home-made instruments or synchrotron facilities [3] but the development of commercial SXES spectrometers (e.g., [4]) has stimulated the use of this technique in existing electron beam instruments, allowing measurements at micron-scale resolution. Despite the number of studies investigating the electronic structure of Ni silicides [5-17] and Al silicides [18-20] by SXES, there are still some silicide phases for which such information is not available.

* Corresponding author: xavier@ccit.ub.edu

In this study, measurements of the Si and Al L emission spectra of selected Ni silicides and aluminides are presented using an SXES spectrometer. The considered phases are $Ni_{31}Si_{12}$, Ni_2Si, $NiAl_3$, and Ni_2Al_3. While Si and Al L spectra have been previously reported for Ni_2Si [6-7,16-17] and $NiAl_3$ [18], to our knowledge, no combined theoretical and experimental studies have been reported for $Ni_{31}Si_{12}$ and Ni_2Al_3.

2 Materials and methods

2.1 Experimental methods

The silicide and aluminide samples were prepared using the diffusion-couple technique, with bulk Ni, Al and Si samples (99.95+% purity) serving as starting metals. The diffusion couples were prepared by hot pressing polished Ni-Si and Ni-Al pieces together and annealing them at 850°C for 16 h (Ni-Si) and 600°C for 60 h (Ni-Al) in a reducing atmosphere. Following annealing, the samples were cross sectioned perpendicular to the interface, through the reaction zone, mounted in epoxy and polished following conventional metallographic procedures. The Ni-Si sample had been prepared in a prior study [21].

The silicide phases were identified by electron probe microanalysis (EPMA). Quantitative analyses were conducted on a JEOL JXA-8230 electron microprobe using a 15 kV accelerating voltage, the Ni Kα, Al Kα and Si K X-ray lines, pure element standards for Al, Ni and Si, and the XPP matrix correction [22].

In the Ni-Si sample, a needle microstructure growing from Ni toward Si perpendicularly to the Ni/Si interface is formed where the $Ni_{31}Si_{12}$, Ni_2Si, Ni_3Si_2, and NiSi phases can be identified, in agreement with published diffusion studies [23-24]. The $Ni_{31}Si_{12}$ and Ni_2Si phases were selected for the SXES measurements. We note here that in [20] the $Ni_{31}Si_{12}$ phase was identified as Ni_5Si_2 (Ni 83.9 wt.%, Si 16.1 wt.%) but re-evaluation of the data suggests that the measured EPMA composition is more consistent with that of $Ni_{31}Si_{12}$. Moreover, according to [24], $Ni_{31}Si_{12}$ is more stable than Ni_5Si_2. Figure 1 (left) displays the appearance of the Ni–Si diffusion-couple cross-section, showing the $Ni_{31}Si_{12}$ and Ni_2Si phases (the needle structure is only visible at lower magnification [23]). A comparison of the nominal and measured compositions for these phases is listed in Table 1.

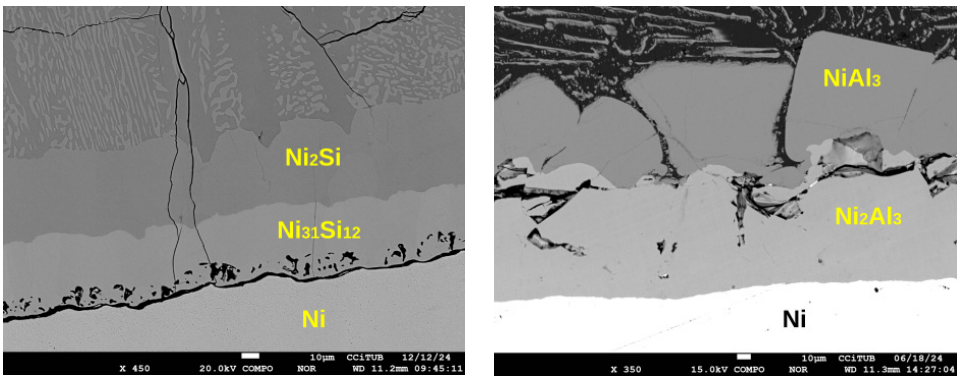

Fig 1. Backscattered electron image of the Ni-Si (left) and Ni-Al (right) diffusion samples showing the studied silicides.

Table 1. Nominal and measured composition of Ni silicides. Results are the average of 10 analyses; standard deviation in parenthesis.

	Nominal concentration (wt.%)		Measured concentration (wt.%)		
Phase	Ni	Si	Ni	Si	Total
$Ni_{31}Si_{12}$	84.38	15.62	84.2 (0.2)	15.6 (0.04)	99.8
Ni_2Si	80.7	19.3	80.9 (0.2)	19.1 (0.05)	100.0

In the Ni-Al sample, two main phases were identified: Ni_2Al_3 and $NiAl_3$, which is also consistent with published Ni-Al diffusion studies (see e.g. [25]). The Ni_2Al_3 phase forms a layered structure with planar interface and the $NiAl_3$ phase forms discrete island-like structures (Fig. 1, right panel). The composition of the Al silicides is summarized in Table 2.

Table 2. Nominal and measured composition of Al silicides. Results are the average of 10 analyses; standard deviations in parenthesis.

	Nominal concentration (wt.%)		Measured concentration (wt.%)		
Phase	Ni	Al	Ni	Al	Total
Ni_2Al_3	59.19	40.81	58.3 (0.4)	41.0 (0.4)	99.3
$NiAl_3$	42.04	57.96	42.0 (0.2)	57.9 (0.4)	99.9

SXES spectra were collected on a JEOL JXA-8230 electron microprobe equipped with an SXES spectrometer. The spectrometer consists of two aberration-corrected, laminar-type, varied-line-spacing diffraction gratings (with dimensions 50 mm × 30 mm × 10 mm) and a backside-illumination X-ray CCD camera (with 2048 × 2048 pixels). The JS50XL grating was used. This grating spans the energy range 48−170 eV and has a groove number of 1200 line/mm [26]. The spectral resolution, as determined by measuring the width of the Fermi edge for metallic Al, was 0.13 eV at 72 eV. X-ray emission was excited by a 5 kV, 200 nA electron beam. Total acquisition time for each spectrum, which was measured at one single location, was 10-15 min. SXES spectra for Si, Al and Ni pure element standards were also measured.

2.2 Computational methods

Density functional theory (DFT) calculations were performed using the all-electron linearized augmented plane wave method, in conjunction with Perdew-Burke-Ernzerhof (PBE) functional in the WIEN2k *ab initio* simulation package [27]. This package allows obtaining the total density of states (DOS), the local DOS (i.e., the DOS around a given element) and the partial DOS (i.e., the DOS with a given symmetry). From the local and partial DOS corresponding to the valence states involved in the transition, X-ray emission spectra are obtained using the electric dipole approximation. The spectra are referenced to the Fermi energy of each compound.

From the calculated DOS, Si (Al) L emission bands ($3sd$ – $2p$ transition) were obtained by using the locally and partially occupied Si (Al) $3s$ and $3d$ valence states. The calculated spectra were broadened by a combination of Lorentzian and Gaussian distributions to simulate the lifetime broadening of both the core and valence states [3] and the experimental

resolution. In particular, we applied a 0.05 eV (0.04 eV) Lorentzian broadening to simulate the Si (Al) *2p* core hole lifetime [28]; a 0-1 eV variable Lorentzian broadening to account for the lifetime of the valence states and a 0.13 eV Gaussian instrumental broadening for the Si (Al) L range.

Calculations were performed for the following materials (in parenthesis the space group): δ–Ni_2Si (*Pbnm*), θ–Ni_2Si (*P6322*), γ–$Ni_{31}Si_{12}$ (*P321*), Ni_2Al_3 (*P-3m1*) and $NiAl_3$ (*Pnma*) whose crystalline structure was obtained from the Inorganic Crystal Structure Database ICSD (https://icsd.fiz-karlsruhe.de).

3 Results and discussion

Si and Al $L_{2,3}$ X-ray emission spectra are produced when core holes generated by electron impact in the 2*p* level are filled by radiative transitions from valence band states. Because of the selection rules, they reflect the distribution of the *s*- and *d*-states in the valence band, in the vicinity of the atom with the core hole.

Figure 2 (left panel) shows the Si $L_{2,3}$ spectra of the Ni silicides, along with that of pure Si. In the case of the silicides, a low-energy peak at around ~90 eV and a broad shoulder extending up to ~100 eV is observed. The low energy peak is slightly wider and shifted to higher energies for Ni_2Si. The structure of the broad shoulder that extends up to ~100 eV is similar for both silicides. A good qualitative agreement is observed for Ni_2Si when comparing with the measurements of Nakamura et al. [6-7], Jarrige et al. [16] and Achuda et al. [17]. In the case of pure Si, the low energy peak splits into two peaks at around ~89.7 eV and ~92.7 eV, and the shoulder extending up to the Fermi edge decreases less rapidly than in the case of the silicides.

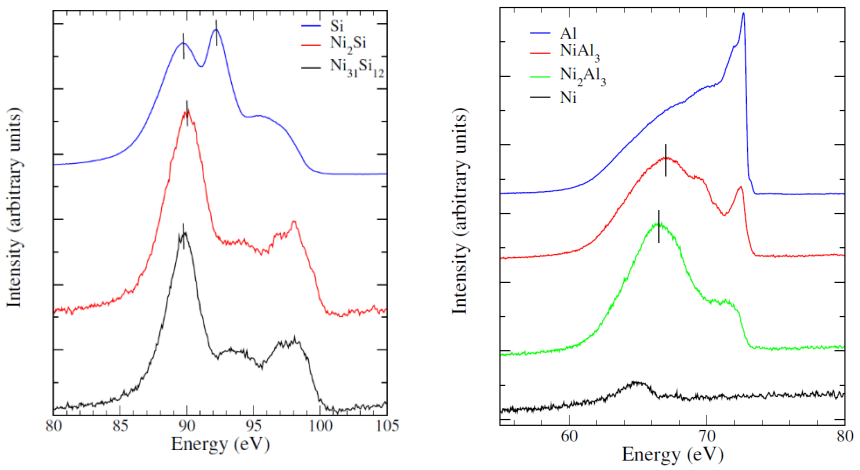

Fig 2. Experimental Si and Al $L_{2,3}$ spectra of Si, Ni_2Si and $Ni_{31}Si_{12}$ (left) and Al, $NiAl_3$, Ni_2Al_3 and Ni (right).

Figure 2 (right panel) compares the Al L spectra of the Al aluminides with that of pure Al and with the Ni $M_{2,3}$ emission spectrum of pure Ni. Although the energy regions of the Al $L_{2,3}$ and Ni $M_{2,3}$ emission spectra overlap, some general remarks can be made. In general, the spectra change considerably with the transition from pure Al to the aluminides. The spectrum of pure Al has a sharp peak structure below the Fermi edge (at around ~72 eV). This peak is also observed for the Ni aluminides but with an intensity falling off with decreasing Al content. A relatively broad peak is observed at ~66.9 eV for $NiAl_3$ and at ~ 66.5 for Ni_2Al_3.

This peak is not observed for pure Al. Our results for $NiAl_3$ resemble the measurements of Cuthill et al. [18].

To allow meaningful comparison of the experimental spectra with the DFT calculations, the experimental spectra were corrected for continuum background, which was fitted as a straight line and subtracted from the spectra, divided by the cube of the photon energy [3], and set on a binding-energy scale relative to the Fermi level E_F. The latter was done by using Si and Al 2*p* core level binding energies from published X-ray photoemission spectroscopy (XPS) experiments on the same materials (99.4 eV for Ni_2Si [29] and 78.9 eV for $NiAl_3$ [30]). Due to the lack of binding energies for $Ni_{31}Si_{12}$ and Ni_2Al_3, the spectra for these materials were tentatively shifted so as to match the DFT calculations at E_F. To facilitate comparison, both the experimental and calculated spectra were normalized to their corresponding maxima. The variation CCD quantum efficiency with photon energy was corrected by using information provided by the manufacturer (Fig. 3). We note here that no attempt was made to correct for self-absorption in the sample, satellite emission and grating reflectance.

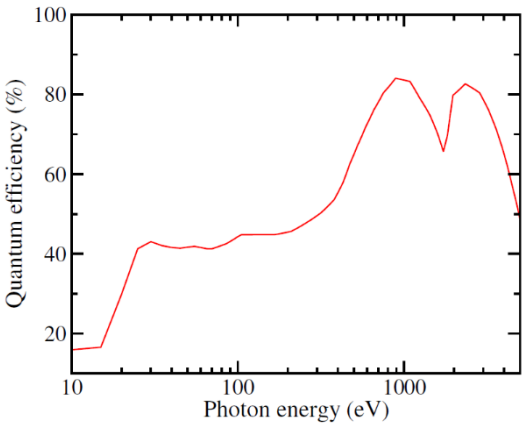

Fig 3. Variation of the CCD quantum efficiency with photon energy

Figure 4 compares the DFT calculated Si L emission bands of Ni_2Si and $Ni_{31}Si_{12}$ with the corresponding experimental spectra. We note here that in the case of Ni_2Si, two phases were modelled, namely δ–Ni_2Si and θ-Ni_2Si. We found a much better agreement of the spectrum modelled as δ-Ni_2Si with our experimental spectrum, which is consistent with this phase being the most stable according to [24]. From the obtained local DOS for Si (not shown here), it is seen that the shape of the Si L spectra is mainly determined by *s*-states; *d*-states are only revealed as the small peak structure in the range 0-5 eV below the Fermi level. Good agreement is generally observed between the calculated and the experimental spectra. The spectral features (marked with arrows) observed along the shoulder extending up to the Fermi edge are generally reproduced in the calculated spectra at the correct positions, although their strength is much higher than that observed in the experiments. This could be in part due to electron correlations with Ni 3*d* electrons, whose description by DFT is difficult, or to the inaccuracy of the experimental corrections that must be made to the emission spectra. The abrupt decay at the Fermi edge indicates the metallic nature of the chemical bond of the Ni silicides.

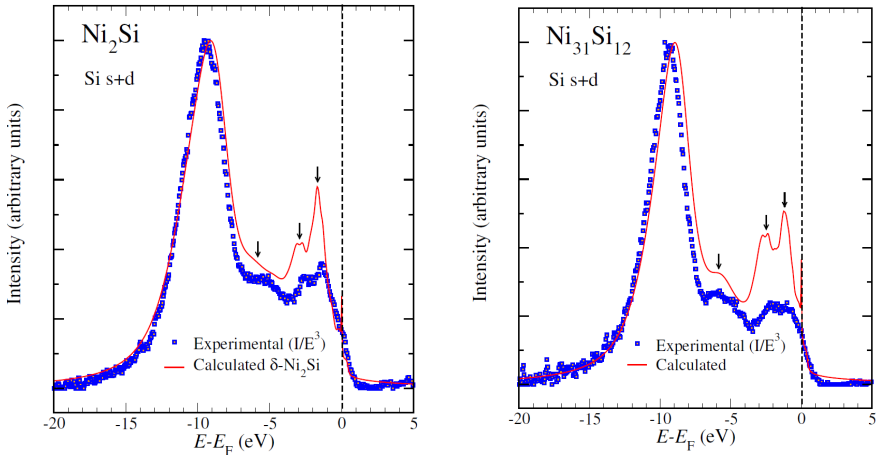

Fig 4. Experimental and calculated Si L spectra for Ni_2Si (left) and $Ni_{31}Si_{12}$ (right).

For $NiAl_3$ and Ni_2Al_3 there is a general resemblance between the calculated and the experimental spectra (Fig. 5), for which the spectral features near the Fermi edge (marked with arrows) are well reproduced by the DFT calculations. However, the main broad peaks of the calculated spectra appear to be stretched and shifted towards higher energies. For these materials, the contribution of the *d*-states extends along the whole bandwidth, with a strength increasing up to the Fermi level (not shown here).

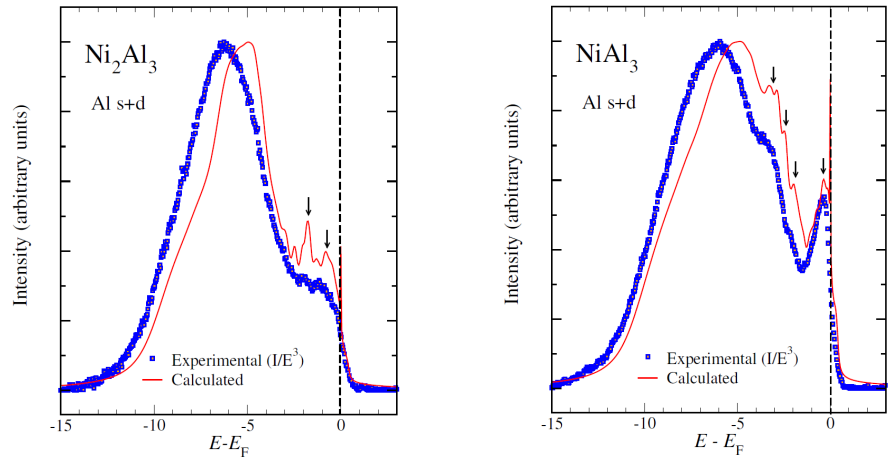

Fig 5. Experimental and calculated Al L spectra for Ni_2Al_3 (left) and $NiAl_3$ (right).

4 Conclusions

We have performed measurements and calculations of Si and Al L X-ray emission spectra for selected Ni silicides and Ni aluminides. The DFT calculated spectra generally resemble the experimental spectra, reproducing the bandwidth and spectral features, although the agreement regarding the position and strength of the latter can only be considered moderate. Work is in progress to improve the experimental corrections that must be made to the emission spectra as well as to extend the study to other silicide materials.

This research was financially supported by Spanish grant PID2023-147788OB-I00 funded by MCIN/AEI/10.13039/501100011033. We thank Tomasz Marzec and Shogo Koshiya for providing us with the CCD quantum efficiency data.

References

1. L. Miglio, F. d'Heurle. Silicides: Fundamentals and Applications (World Scientific, Singapore, 2000)
2. S. Sampath, V.P. Ravi, S. Sundararajan. An overview on synthesis, processing and applications of nickel aluminides: from fundamentals to current prospects. Crystals **13**, 435 (2023) https://doi.org/10.3390/cryst13030435
3. D.J. Fabian. Soft X-ray band spectra. (Academic Press, London, 1968)
4. M. Terauchi, Y. Yamamoto, M.D. Tanaka. Development of a sub-eV resolution soft-X-ray spectrometer for a transmission microscope. J. Electron Microsc. **50**, 101 (2001) https://doi.org/10.1093/jmicro/50.2.101
5. P.J.W. Weijs, G. Wiech, W. Zahorowski, W. Speiep, J.B. Goedkoop, M. Czyzyk, J.F. van Acker, E. van Leuken, R.A. de Groot, G. van der Laan, D. D. Sarma, L. Kumar, K. H. J. Buschow, J. C. Fuggle. X-ray emission and absorption studies of silicides in relation to their electronic structure. Phys. Scr. **41**, 629 (1990) https://doi.org/10.1088/0031-8949/41/4/056
6. H. Nakamura, M. Iwami, M. Hirai, M. Kusaka, F. Akao, H. Watabe. Valence-band electronic structure of $NiSi_2$ and $CoSi_2$. Evidence of the Si s electronic state at the Fermi edge. Phys. Rev. B **41,** 12092 (1990) https://doi.org/10.1103/PhysRevB.41.12092
7. H. Nakamura, M. Hirai, M. Kusaka, M. Iwami, H. Watabe. Soft X-ray spectroscopic analysis of Ni-Silicides. J. Phys. Soc. Jap. **61,** 616 (1992) https://doi.org/10.1143/JPSJ.61.616
8. P.J.W. Weijs, H.V. Leuken, R.A. Groot, J.C. Fuggle, S. Reiter, G. Wiech, K.H.J. Buschow. X-ray-emission studies of chemical bonding in transition-metal silicides. Phys. Rev. B **44,** 8195 (1991) https://doi.org/10.1103/PhysRevB.44.8195
9. J.J. Jia, T.A. Callcott, W.L. O'Brien, Q.Y. Dong, J.E. Rubensson, D. R. Mueller, D.L. Ederer, and J.E. Rowe. Local partial densities of states in Ni and Co silicides studied by soft X-ray emission spectroscopy. Phys. Rev. B **43**, 4863 (1991) https://doi.org/10.1103/PhysRevB.43.4863
10. J.J. Jia. Bonding in transition-metal silicides studied via soft-x-ray-emission spectroscopy. PhD diss., University of Tennessee (1991) https://trace.tennessee.edu/utk_graddiss/11140
11. E.Z. Kurmaev, V.V. Fedorenko, S.N. Shamin and A.V. Postnikov. Small-spot X-ray emission spectroscopy and its application for study of electronic structure and chemical bonding in solids. Phys. Scr. **T41**, 288 (1992) https://doi.org/10.1088/0031-8949/1992/T41/052
12. S. Yamauchi, S. Kawamoto, M. Hirai, M. Kusaka, M. Iwami, H. Nakamura, H. Ohshima, T. Hattori. Valence-band density of states of near-noble-metal (Ni, Pd, Pt) monosilicides by using soft-x-ray-emission spectroscopy. Phys. Rev. B **50**, 11564 (1994) https://doi.org/10.1103/PhysRevB.50.11564
13. A. Kinoshita, M. Hirai, M. Kusaka, M. Iwami. Si L_{23} soft X-ray emission spectra by quantitative analyis of silicides/Si system: simulation and experiment. J. Surf. Anal. **5**, 86 (1999).

14. N.S. Pereslavtseva, S.I. Kurganskii. Electronic structure and spectral properties of nickel disilicide films. Phys. Sol. Stat. **41**, 1906 (1999) https://doi.org/10.1134/1.1131124
15. N.S. Pereslavtseva, S.I. Kurganskii. Theoretical photoemission and X-ray emission spectra of nickel and cobalt disilicide films. J. Electron. Spectros. Relat. Phenom. **114-116**, 549 (2001) https://doi.org/10.1016/S0368-2048(00)00345-5
16. I. Jarrige, N. Capron, P. Jonnard, Electronic structure of Ni and Mo silicides investigated by X-ray emission spectroscopy and density functional theory. Phys. Rev. B **79,** 035117 (2009) https://doi.org/10.1103/PhysRevB.79.035117
17. G. Achuda, H. Löchel, J. Probst, A. Erko, C. Seifert, T. Krist, S. Richter. Investigating the soft X-ray emission spectra of nickel silicides in EPMA. EMAS-2023 Book of Tutorial and Abstracts, p. 288 (EMAS, Zürich, 2023). ISBN 978 90 8277 6961
18. J.R. Cuthill, A.J. McAlister, M.L. Williams. Soft X-ray spectroscopy of alloys: TiNi and the Ni–Al System. J.Appl.Phys. **39,** 2204 (1968) https://doi.org/10.1063/1.1656528
19. K. Ichikawa. The soft X-ray emission spectra of the aluminium transition metal alloys. J. Phys. Soc. Jap. **37**, 377 (1974) https://doi.org/10.1143/JPSJ.37.377
20. S.B. Maslenkov, A.I. Kozlenkov, S.A. Filln, A.I. Shulg. Soft X-ray emission spectra from some Ni-A1 alloys. Phys. Stat. Sol. (b) **123**, 605 (1984) https://doi.org/10.1002/pssb.2221230224
21. X. Llovet, P.T. Pinard, E. Heikinheimo, S. Louhenkilpi, S. Richter, Electron Probe Microanalysis of Ni Silicides Using Ni-L X-ray lines, Microsc. Microanal. **22**, 1233 (2016) https://doi.org/10.1017/S1431927616011831
22. J.L. Pouchou, F. Pichoir. Quantitative analysis of homogeneous or stratified microvolumes applying the model "PAP." In: K.F.J Heinrich, D.E. Newbury, editors. Electron Probe Quantitation, p. 31-75 (Springer, New York, 1991)
23. D. Borivent, B. Billia, J. Paret. Anomalous growth of Ni3Si2 in bulk Ni/Si interdiffusion. J. Appl. Phys. **104**, 013523 (2008) https://doi.org/10.1063/1.2946721
24. D. Connétable, O. Thomas. Olivier First-principles study of nickel-silicides ordered phases. J. Alloys Compd. **509** 2639 https://doi.org/10.1016/j.jallcom.2010.10.118
25. C. Li, Z. Yuan, R. Guo, W. Xuan, Z. Ren, Y. Zhong, X. Li, H. Wang, Q. Wang. Reaction diffusion in Ni–Al diffusion couples in steady magnetic fields. J. Alloy. Compd. **641**, 7 (2015) https://doi.org/10.1016/j.jallcom.2015.04.061
26. T. Imazono, M. Koike, T. Kawachi, N. Hasegawa, M. Koeda, T. Nagano, H. Sasai, Y. Oue, Z. Yonezawa, S. Kuramoto, M. Terauchi, H. Takahashi, N. Handa, T. Murano, K. Sano. Laminar and blazed type holographic gratings for a versatile soft x-ray spectrograph attached to an electron microscope and their evaluation in the 50–200 eV range. Apl. Opt. **51**, 2351 (2012) https://doi.org/10.1364/AO.51.002351
27. P. Blaha, K. Schwarz, F. Tran, R. Laskowski, G.K.H. Madsen, L.D. Marks, WIEN2k: An APW+lo program for calculating the properties of solids. J. Chem. Phys. **152**, 074101 (2020) https://doi.org/10.1063/1.5143061
28. J.L. Campbell, T. Papp, Widths of the atomic K-N7 levels. Atom. Data Nucl. Data Tab. **77**, 1 (2001) https://doi.org/10.1006/adnd.2000.0848
29. E.P. Domashevskaya, Y.A. Yurakov. Specific features of electron structures of some thin film d-silicides. J. Electron Spectrosc. Relat. Phenom. **96**, 195 (1998) https://doi.org/10.1016/S0368-2048(98)00236-9

30. N. Ohtsu, M. Oku, T. Shishido, K. Wagatsuma. X-ray photoelectron spectroscopic studies on phase identification and quantification of nickel aluminides. Appl. Surf. Sci. **253,** 8713 (2007) https://doi.org/10.1016/j.apsusc.2007.04.049